substance: NiO
property: optical properties, dielectric constants

optical spectra: photoemission: Fig. 2; XPS: Fig. 5; absorption: Figs. 6...9; electroreflectance: Fig. 10; thermoreflectance: Fig. 11; real and imaginary parts of the refractive index: Fig. 12, of the dielectric constant: Fig. 1.

For the photoemission spectra (Fig. 2) two interpretations in terms of local cluster-type calculations are given (Fig. 3). Interpretation in terms of a band structure calculation: Fig. 4. The O 2p band is ≈ 5 eV wide but the width of the 3d signals may not represent the true bandwidth. A finite signal width would be expected even in the zero-overlap limit arising from vibronic effects. The core region XPE spectrum (Fig. 5) shows two satellites on Ni $2p_{3/2}$ which have been assigned to Ni d–d or multiplet splitting (1.8 eV) and O 2p → Ni 3d (6.0 eV) [74K]. From [73H] the value of the Hubbard self-energy *U* has been estimated as 1...3 eV. The 6.0 eV peak does not correspond to the minimum O 2p → 3d energy since selection rules will favour the O 2p ($e_g\sigma$) → Ni 3d ($e_g\sigma^*$) transition [74K].

Electroreflectance spectra (Fig. 10) show pronounced structure at the optical threshold (3.5 eV). The assignment of the optical edge at 3.5 eV is controversial, with $d^8 \rightarrow d^7s$ [70P, 72M], O 2p → Ni d^9 [78M, 81D] and 2 Ni d^8 → Ni d^9 +Ni d^7 [76A] all suggested. Problems with all these assignments have been noted. Assignments of the EELS spectrum is also difficult, though the weight of evidence would suggest O 2p – Ni 3d at 4.6 and 6.9 eV and O2p – Ni 4s at 9.5 and 11.7 eV [77S].

refractive index

n	2.26	RT	in the visible, see also Fig. 12	58D
	2.33			70P
	2.38			65G

dielectric constants

$\varepsilon(0)$	11.75	RT	65G
	13.0		75R
$\varepsilon(\infty)$	5.70		65G
	5.7		75R

References:

58D Doyle, W. P., Lonergan, G. A.: Discuss. Faraday Soc. 26 (1958) 27.
59N Newman, R., Chrenko, R. M.: Phys. Rev. 114 (1959) 1507.
65G Gielisse, P. J., Plendl, J. N., Mansur, L. C., Marshall, R., Mitra, S. S., Mykolojewicz, R., Smakula, A.: J. Appl. Phys. 36 (1965) 2446.
69M McNatt, J. L.: Phys. Rev. Lett. 23 (1969) 915.
70B Bosman, A. J., van Daal, H. J.: Adv. Phys. 19 (1970)1.
70P Powell, R. J., Spicer, W. E.: Phys. Rev. B2 (1970) 2182.
71G Glosser, R., Walker, W. C.: Solid State Commun. 9 (1971) 1599.
72M Messick, L., Walker, W. C., Glosser, R.: Phys. Rev. B6 (1972) 3941.
72W Wertheim, G. K., Hüfner, S.: Phys. Rev. Lett. 23 (1972) 1028.
73H Hüfner, S., Wertheim, G. K.: Phys. Rev. B8 (1973) 4857.
73J Johnson, K. H., Messmer, R. P., Lonnolly, J. W. D.: Solid State Commun. 12 (1973) 313.
74K Kim, K. S.: J. Electron Spectrosc. Rel. Phenom. 3 (1974) 217.
75C Cerdeira, F., Holzapfel, W.B., Bauerle, D.: Phys. Rev. 11 (1975) 1188.
75E Eastman, D. E., Freeouf, J. L.: Phys. Rev. Lett. 34 (1975) 395.
75R Reichardt, W., Wagner, V., Kress, W.: J. Phys. C8 (1975) 3955.
76A Allen, G. C., Dyke, J. M.: Chem. Phys. Lett. 37 (1976) 391.
77S Sakisaki, Y., Akimoto, K., Nichijima, M., Onchi, M.: Solid State Commun, 24 (1977) 105.
78K Kunz, A. B., Surratt, G. T.: Solid State Commun. 25 (1978) 9.
78M Merlin, R., Martin, T. P., Polian, A., Cardona, M., Audlauer, B., Tannhauser, D.: J. Magnetism Magn. Mater. 9 (1978) 83.
78P Propach, V., Reinen, D., Drenkhahn, H., Müller-Buschbaum, H.: Z. Naturforsch. 33B (1978) 619.
81D Dare-Edwards, M. P., Goodenough, J. B., Hamnett, A., Nicholson. N. D.: Faraday Trans. Chem. Soc. II 77 (1981) 643.

Figures:

Fig.1.

NiO:Na. (a) Real part of the dielectric constant vs. temperature for different frequencies for a sample doped with 0.1 at% Na. The broken line represents the behaviour of $\varepsilon(0)$ if $\Delta\varepsilon$ is proportional to T^{-1}, (b) imaginary part of the dielectric constant vs. frequency for different temperatures measured on the same crystal as in (a). The broken line represents a Debye curve with its maximum at 10^7 Hz [70B].

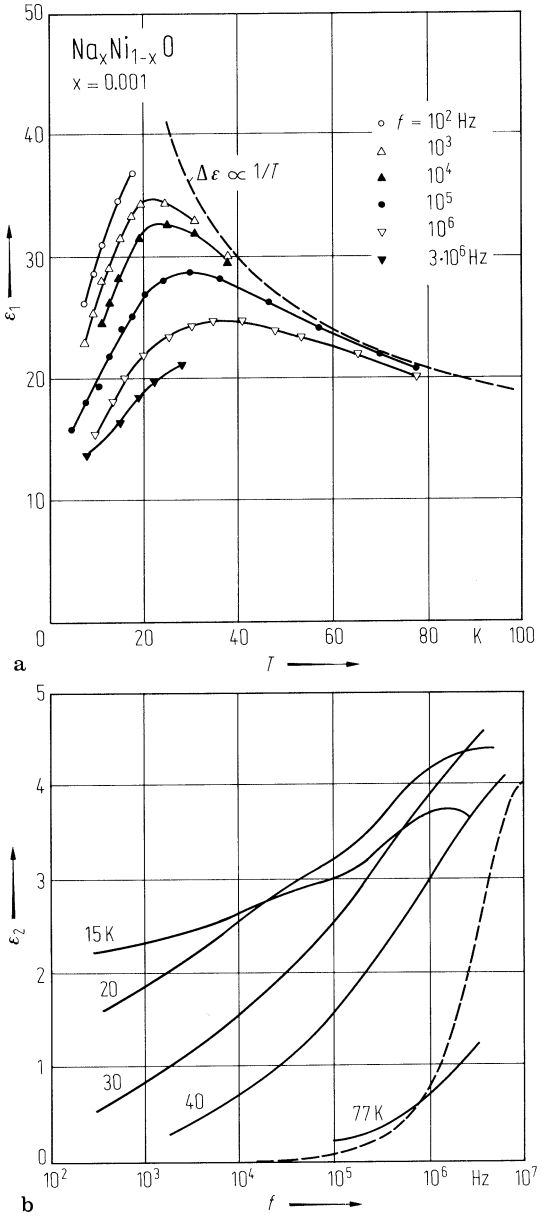

Fig. 2.

NiO. Photoemission spectrum (intensity vs. electron binding energy relative to the d-peak) at different incident light energies [75E].

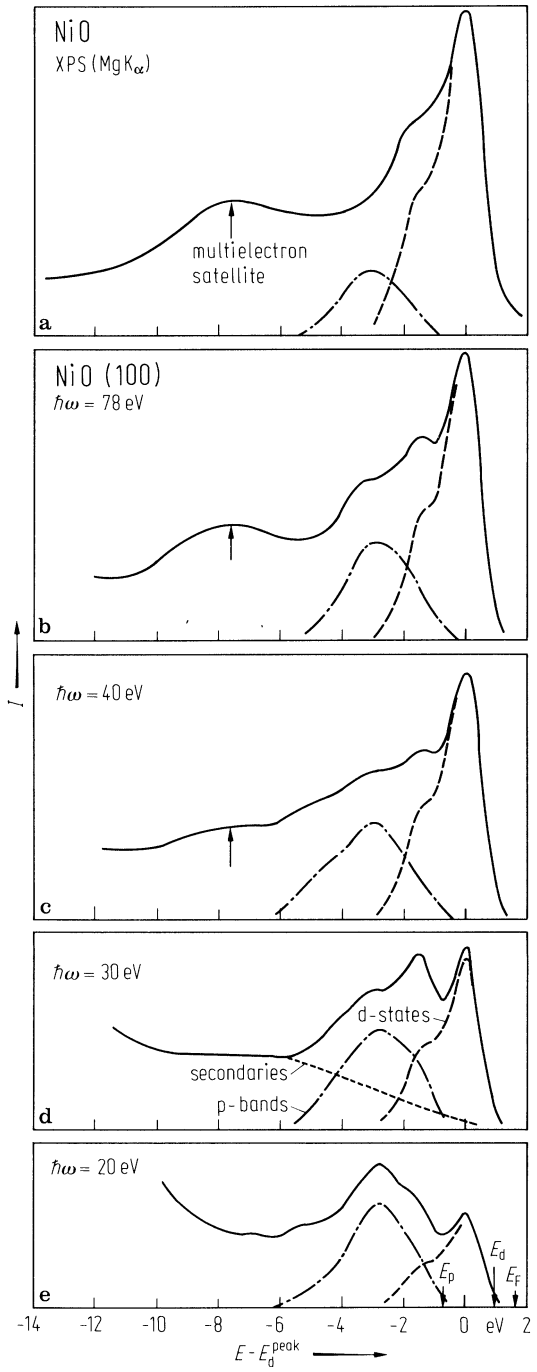

Fig. 3.

NiO. SCF-Xα transition state energies of an NiO_6^{10-} cluster superimposed on the NiO XPS-data of [72W]. Only the spin polarization of predominantly 3d-like levels is indicated. E_b is relative to the experimental Fermi energy of the spectrometer [73J, 75E].

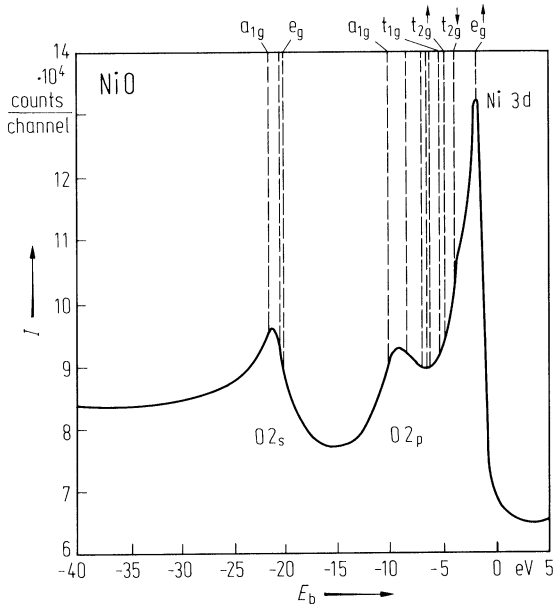

Fig. 4.

NiO. Band calculations (a) [78K], (b) [72M], (c) [75C] along the ΓX-axis in *k*-space; (d) comparison with the experimental density of states from photoemission spectra [78K].

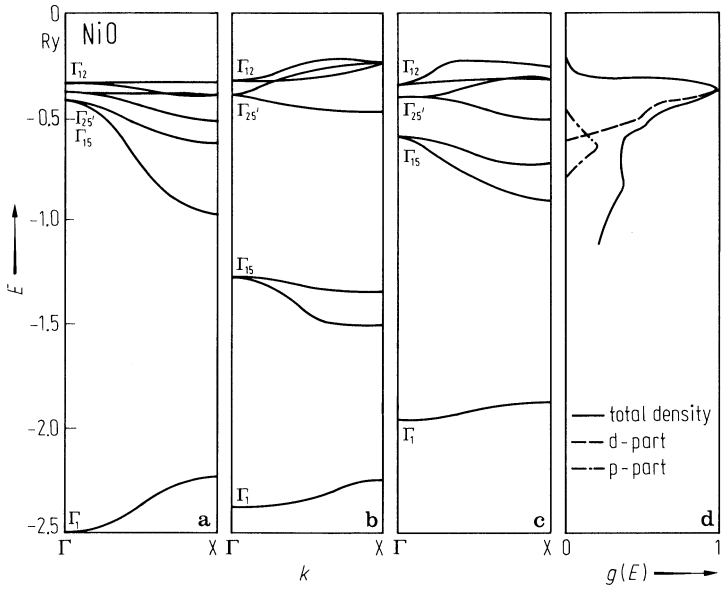

Fig. 5.

NiO. XPS spectra. Intensity vs. electron binding energy relative to zero of Fig. 3 of the Ni(2p) and O(1s) regions [72W]. sat. = satellite.

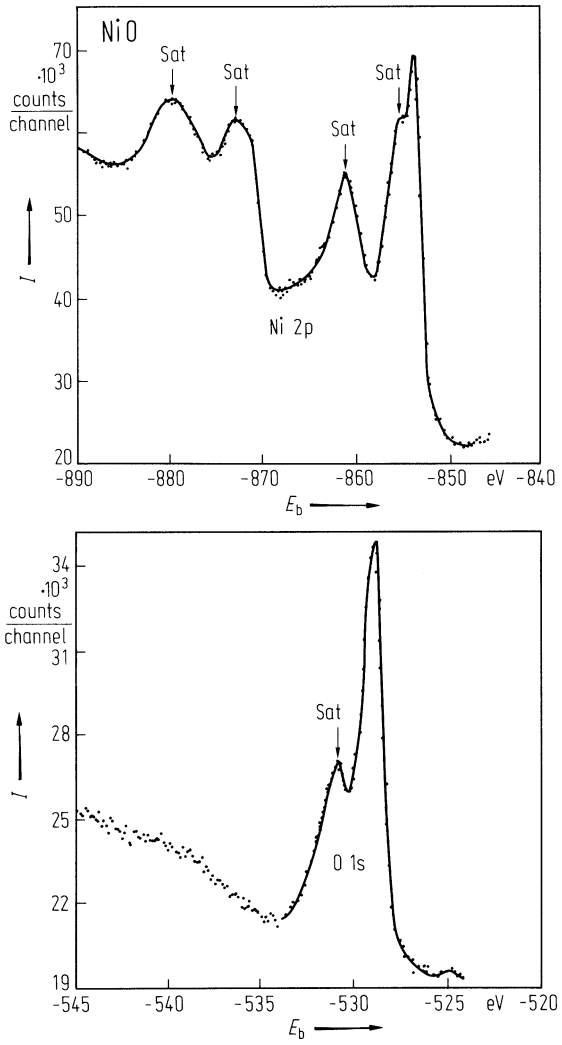

Fig. 6.

NiO. Absorption coefficient vs. photon energy [70P].

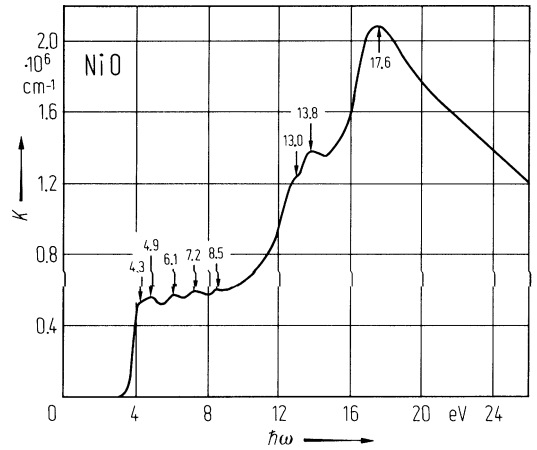

Fig. 7.

NiO. Optical density vs. photon energy (wavelength) showing details of the absorption edge [70P].

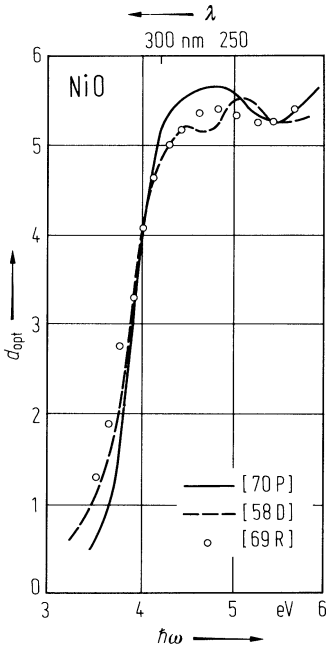

Fig. 8.

NiO. Absorbance (log *k*/*s*) vs. wavenumber. Assignment in terms of local exciton formation is given [78P]. *k*: absorbed radiant flux, *s*: incident radiant flux.

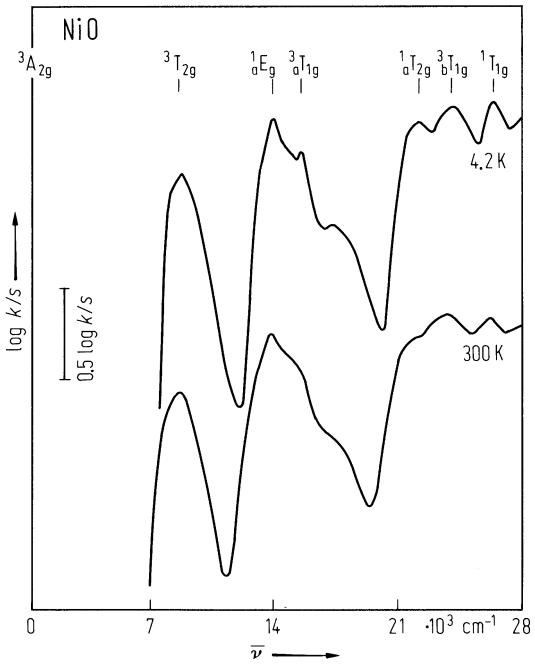

Fig. 9.

NiO. Optical density vs. photon energy in the region of the 0.24 eV absorption peak for various temperatures. The peak has been assigned to a two-magnon and one phonon excitation [59N]. $d_{opt} = \log(I_0/I)$.

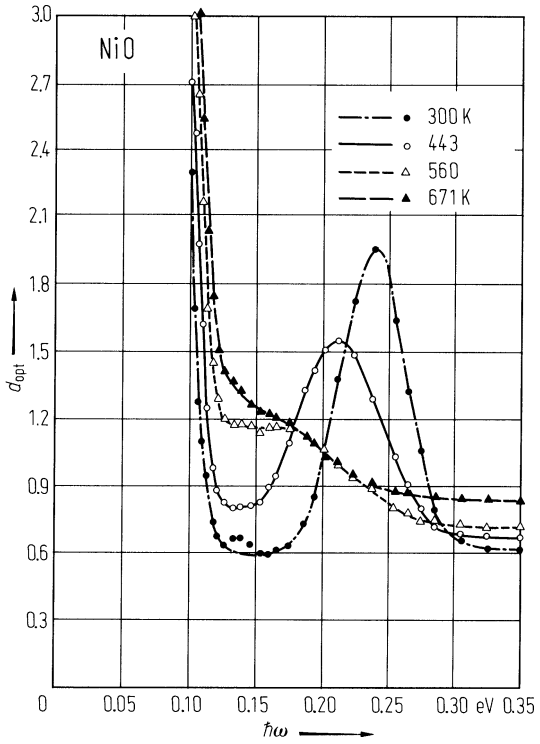

Fig. 10.

NiO. Electroreflectance spectrum (electroreflectance vs. photon energy and wavelength) [71G, 69M].

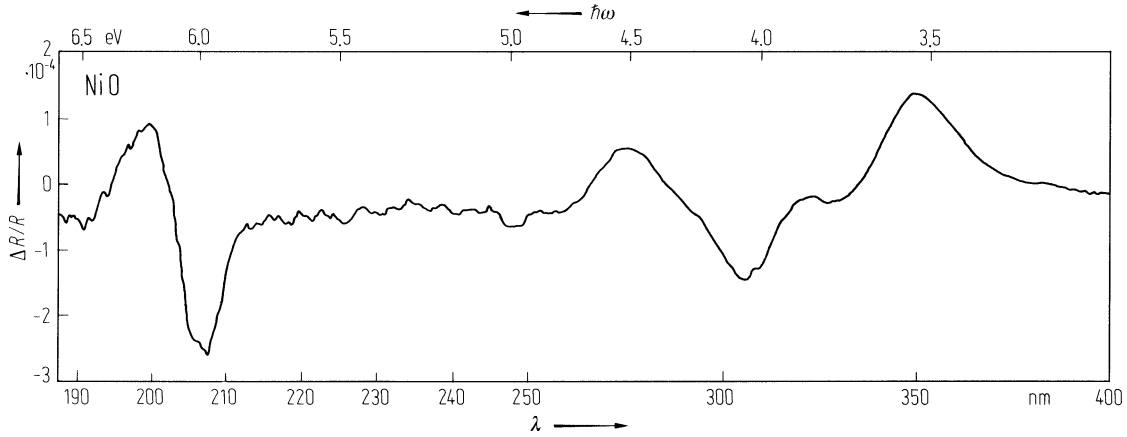

Fig. 11.

NiO. Thermoreflectance vs. photon energy and wavelength [72M].

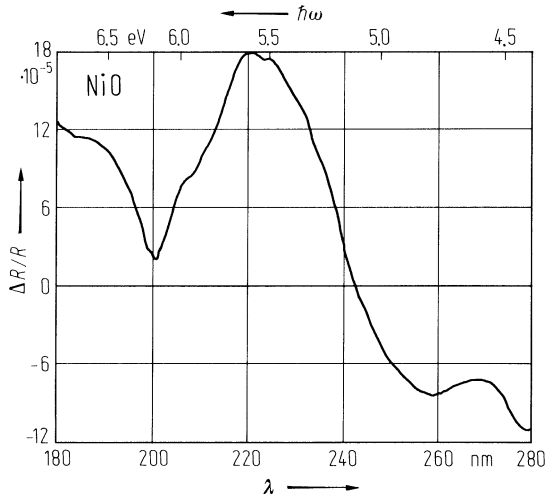

Fig. 12.

NiO. Real and imaginary parts of the complex refractive index vs. photon energy [70P].